



CHORUS

This is the accepted manuscript made available via CHORUS. The article has been published as:

Improving Band Gap Prediction in Density Functional Theory from Molecules to Solids

Xiao Zheng, Aron J. Cohen, Paula Mori-Sánchez, Xiangqian Hu, and Weitao Yang

Phys. Rev. Lett. **107**, 026403 — Published 7 July 2011

DOI: [10.1103/PhysRevLett.107.026403](https://doi.org/10.1103/PhysRevLett.107.026403)

Improving band gap prediction in density functional theory from molecules to solids

Xiao Zheng,¹ Aron J. Cohen,² Paula Mori-Sánchez,³ Xiangqian Hu,¹ and Weitao Yang¹

¹*Department of Chemistry, Duke University, Durham, North Carolina 27708*

²*Department of Chemistry, Lensfield Road,*

University of Cambridge, Cambridge, CB2 1EW, United Kingdom

³*Departamento de Química, Universidad Autónoma de Madrid, 28049 Madrid, Spain*

Abstract

A novel nonempirical scaling correction (SC) method is developed to tackle the challenge of band gap prediction in density functional theory. For finite systems the SC largely restores the straight-line behavior of electronic energy at fractional electron numbers. The SC can be generally applied to a variety of main-stream density functional approximations, leading to significant improvement on band gap prediction. In particular, the scaled version of a modified localized density approximation (MLDA) predicts band gaps with an accuracy consistent for systems of all sizes, ranging from atoms and molecules to solids. The scaled MLDA thus provides a useful tool to quantitatively characterize the size-dependent effect on the energy gaps of nanostructures.

PACS numbers: 31.15.E-, 71.10.-w, 71.15.Mb

Accurate prediction of band gaps is one of the critical challenges in density functional theory (DFT) with potential wide applications. The capability to predict gaps for systems of all sizes is critical for study of material interfaces, but currently remains out of reach within DFT.

For a system of N electrons (N is an integer) in an external potential $v(\mathbf{r})$, its fundamental (or integer) band gap is $E_{\text{gap}}^{\text{int}} = I - A$, where $I = E_v(N-1) - E_v(N)$ is the ionization potential, and $A = E_v(N) - E_v(N+1)$ is the electron affinity. With n additional fractional electron ($0 < n < 1$), the system energy as a function of n is given by the Perdew–Parr–Levy–Balduz (PPLB) condition:¹ it is a straight line interpolation between energies at integer points, *i.e.*, $E_v(N+n) = (1-n)E_v(N) + nE_v(N+1)$. Such a linear relation infers that, in principle $E_{\text{gap}}^{\text{int}}$ should be exactly reproduced by the derivative gap, *i.e.*, the difference between left and right energy derivatives at N : $E_{\text{gap}}^{\text{der}} \equiv \lim_{n \rightarrow 0} (\frac{\partial E_v}{\partial N} \Big|_{N+n} - \frac{\partial E_v}{\partial N} \Big|_{N-n}) = E_{\text{gap}}^{\text{int}}$. More specifically, the exact DFT should give $I = -\lim_{n \rightarrow 0} \frac{\partial E_v}{\partial N} \Big|_{N-n}$ and $A = -\lim_{n \rightarrow 0} \frac{\partial E_v}{\partial N} \Big|_{N+n}$.^{1,2}

In the Kohn–Sham (KS) scheme³ where the exchange–correlation (XC) energy is an explicit functional of electron density, *i.e.*, $E_{\text{xc}} = E_{\text{xc}}[\rho(\mathbf{r})]$, it has been proved that $\frac{\partial E_v}{\partial N} = \epsilon_f$, with ϵ_f being the KS frontier orbital energy.² f is either the highest occupied molecular orbital (HOMO) if N is approached from $N-n$, or otherwise the lowest unoccupied molecular orbital (LUMO). Therefore, $E_{\text{gap}}^{\text{der}} = \epsilon_{\text{LUMO}} - \epsilon_{\text{HOMO}}$. The same situation applies to the generalized KS scheme, where $E_{\text{xc}} = E_{\text{xc}}[\rho_s(\mathbf{r}, \mathbf{r}')]]$ with $\rho_s(\mathbf{r}, \mathbf{r}')$ being the KS first-order reduced density matrix. Therefore, if the linearity condition could be satisfied, $I = -\epsilon_{\text{HOMO}}$, $A = -\epsilon_{\text{LUMO}}$, and thus $E_{\text{gap}}^{\text{der}} = E_{\text{gap}}^{\text{int}}$ should be realized in DFT.²

The actual fractional charge behavior of $E_v(N+n)$ of standard density functional approximations (DFAs) is summarized as follows: (i) Local density approximation (LDA) and generalized gradient approximation (GGA) give reasonable I , A , and hence $E_{\text{gap}}^{\text{int}}$ for small systems. However, they predict much too high ϵ_{HOMO} and too low ϵ_{LUMO} , and thus greatly underestimate $E_{\text{gap}}^{\text{der}}$. This is due to the delocalization error, which gives an overall convex energy curve.⁴ (ii) Hartree–Fock (HF) gives less accurate energies at integers, due to the lack of electron correlation. Its significant localization error leads to a rather concave energy curve,⁵ and severe overestimation of $E_{\text{gap}}^{\text{der}}$. (iii) Hybrid and range-separated hybrid DFAs such as B3LYP,⁶ PBE0,⁷ HSE,⁸ and HISS⁹ have both convex and concave ingredients. Delocalization error is generally not compensated by localization error, resulting in a convex energy curve and underestimation of $E_{\text{gap}}^{\text{der}}$.¹⁰ (iv) Self-interaction correction (SIC) of Perdew and

Zunger¹¹ straightens the LDA/GGA energy curve, but significantly degrades the description of integers.¹² (v) Long-range corrected DFAs such as MCY3¹³ and rCAM-B3LYP¹³ achieve the correct straight-line behavior.¹⁴ They yield accurate $E_{\text{gap}}^{\text{int}}$ and $E_{\text{gap}}^{\text{der}}$ for atoms and small molecules, but the error increases significantly as the system size grows. Therefore, none of the existing DFAs is capable of predicting band gaps with consistent accuracy for systems of all sizes.

To fix this problem, we start with a DFA which gives reasonable band gaps for solids, and then improve its prediction on atoms and molecules of all sizes. For bulk systems, the convexity of LDA energy curve is suppressed by infinite system size.⁴ However, delocalization error remains at integers, resulting in significant underestimation of band gaps for nonmetallic solids by LDA. Bylander and Kleinman¹⁵ have combined screened HF exchange with long-range LDA. The resulting DFA, the modified LDA (MLDA), improves the band-gap prediction for semiconductors. They used $\frac{\exp(-K_s r)}{r}$ as the screened Coulomb operator with K_s being a function of $\rho(\mathbf{r})$.¹⁵ A different range separation scheme, $\frac{1}{r} = \frac{\text{erf}(\mu r)}{r} + \frac{\text{erfc}(\mu r)}{r}$, has been popular in the DFT community.^{13,16,17} Here, $\text{erf}(x)$ is the error function and $\text{erfc}(x) = 1 - \text{erf}(x)$. Employing the erf-splitting and VWN5¹⁸ for correlation, we have

$$E_{\text{xc}}^{\text{MLDA}} = E_{\text{x}}^{\text{SR,HF}} + E_{\text{x}}^{\text{LR,LDA}} + E_{\text{c}}^{\text{LDA}}. \quad (1)$$

The form of $E_{\text{x}}^{\text{LR,LDA}}$ is given in Refs. 16 and 19. We choose $\mu = 0.5 \text{ bohr}^{-1}$ as it is within the typical range for screened exchange length.¹⁶ Our calculations clearly indicate MLDA systematically improves over LDA; see Fig. 1. MLDA gives a mean absolute error (MAE) of 0.22 eV for 13 covalent crystals with gaps below 7 eV. For large-gap ionic and noble gas crystals, the error increases with the gap, due to the weaker dielectric screening in these materials. Nevertheless, MLDA still outperforms LDA. For metals MLDA correctly predicts zero gaps.¹⁹ We notice that other approaches have recently been proposed to improve solid band gaps.^{20,21}

Much like LDA, MLDA gives a convex energy curve for atoms and molecules. To achieve accurate $E_{\text{gap}}^{\text{der}}$ for finite systems, it is essential to reduce the delocalization error by restoring the linearity condition. The total electronic energy in DFT is $E_v = T_s + V_{\text{ext}} + J + E_{\text{xc}}$. With the KS orbitals fixed as the electron number is varied, the KS kinetic energy T_s and external potential energy V_{ext} are linear in $\rho(\mathbf{r})$; while the electron Coulomb energy $J[\rho]$ is

quadratic, and $E_{xc}[\rho]$ is usually nonlinear in $\rho(\mathbf{r})$. Therefore, a linear $E_v(N+n)$ can be achieved by linearizing both $J[\rho]$ and $E_{xc}[\rho]$ with respect to n , the main goal of our scaling correction (SC).¹⁹

As the number of electrons increases from N to $N+n$, $\rho(\mathbf{r})$ varies as $\rho_{N+n}(\mathbf{r}) \simeq \rho_N(\mathbf{r}) + nf(\mathbf{r})$, with $f(\mathbf{r}) = \lim_{n \rightarrow 0} \frac{\partial \rho_{N+n}(\mathbf{r})}{\partial n} |_{v(\mathbf{r})}$ being the Fukui function.²² Consider $g(\mathbf{r}) \equiv \int d\mathbf{r}' \rho_s(\mathbf{r}, \mathbf{r}') \rho_s(\mathbf{r}', \mathbf{r}) = \sum_{i \in \text{occ}} n_i^2 |\phi_i(\mathbf{r})|^2$, with $\phi_i(\mathbf{r})$ and n_i being the i th KS orbital and occupation number. At $0 < n < 1$, $\rho(\mathbf{r}) - g(\mathbf{r}) = (n - n^2) |\phi_f(\mathbf{r})|^2$, with $\phi_f(\mathbf{r})$ being the fractionally occupied KS orbital. The square of spinless first-order reduced density matrix has been used for describing the distributions of odd electrons²³ and effectively unpaired electrons.²⁴

The SC to $J[\rho]$ is obtained as¹⁹

$$\begin{aligned} \Delta J(N+n) &= \frac{n - n^2}{2} \iint d\mathbf{r} d\mathbf{r}' \frac{f(\mathbf{r})f(\mathbf{r}')}{|\mathbf{r} - \mathbf{r}'|} \\ &\simeq \frac{1}{2} \iint d\mathbf{r} d\mathbf{r}' \frac{[\rho(\mathbf{r}) - g(\mathbf{r})] |\phi_f(\mathbf{r}')|^2}{|\mathbf{r} - \mathbf{r}'|}. \end{aligned} \quad (2)$$

where $f(\mathbf{r}) \simeq |\phi_f(\mathbf{r})|^2$ is used in the second step. At integer points, $\Delta J = 0$ due to $\rho(\mathbf{r}) = g(\mathbf{r})$. However, $\frac{\partial \Delta J}{\partial n}$ is nonzero at either $n = 0$ or 1 . This nonzero derivative gives a finite correction to ϵ_f and $E_{\text{gap}}^{\text{der}}$.

For the XC energy only the exchange part is treated, since the SC to correlation energy is much smaller. The SC to exchange energy, ΔE_x^{DFA} , can be obtained by exploring the scaling relation of exchange energy at fractional electron occupation. We derive the form of ΔE_x^{DFA} for a variety of main-stream DFAs, including LDA, GGA, hybrid functional B3LYP, and range-separated functional MLDA. The detailed derivations are provided in Ref. 19. For all the DFAs investigated, the SC contribution to exchange energy takes the following generic form:

$$\Delta E_x^{\text{DFA}} = \int d\mathbf{r} [\rho(\mathbf{r}) - g(\mathbf{r})] \theta_x^{\text{DFA}}(|\phi_f|^2; \mathbf{r}). \quad (3)$$

Here, the function $\theta_x^{\text{DFA}}(\mathbf{r})$ depends explicitly on $|\phi_f(\mathbf{r})|^2$. We emphasize that the form of θ_x^{DFA} is nonempirical (free of any fitted parameter) for LDA, GGA, and B3LYP. Combining Eqs. (2)–(3), the XC energy associated with a scaled DFA (S-DFA) is thus

$$E_{xc}^{\text{S-DFA}} = E_{xc}^{\text{DFA}} + \Delta J + \Delta E_x^{\text{DFA}}. \quad (4)$$

This is the central result of this work. Specifically,

$$\theta_x^{\text{MLDA}}(\mathbf{r}) = -\frac{1}{2} \int d\mathbf{r}' \left[\frac{|\phi_f(\mathbf{r}')|^2 \operatorname{erfc}(\mu|\mathbf{r}-\mathbf{r}'|)}{|\mathbf{r}-\mathbf{r}'|} \right] - \alpha_\mu C_x |\phi_f(\mathbf{r})|^{\frac{2}{3}}, \quad (5)$$

with $C_x = \frac{3}{4} \left(\frac{6}{\pi}\right)^{\frac{1}{3}}$. We choose the semiempirical parameter $\alpha_\mu = 0.22222$ at $\mu = 0.5 \text{ bohr}^{-1}$.¹⁹

Although the self-consistent-field (SCF) process inevitably alters the KS orbitals and modifies the scaling relation of each energy component, the scaling relation of total electronic energy is largely maintained. This is validated by the fact that a scaled DFA generally yields a much more straight energy curve than that by the original DFA,¹⁹ which also confirms that the SC significantly reduces the delocalization error associated with a convex DFA.⁴ At an integer point, the SC vanishes due to $\rho(\mathbf{r}) = g(\mathbf{r})$. Consequently, the S-DFA reproduces I , A , and $E_{\text{gap}}^{\text{int}}$ of the original DFA, while it improves significantly the prediction on ϵ_f and $E_{\text{gap}}^{\text{der}}$. We emphasize that virtually no extra computational cost is required for the evaluation of the SC-related quantities, and the SC method can be easily implemented in existing quantum chemistry softwares; see Sec. IE of Ref. 19 for details.

For molecules it is the vertical I (I_{ve}) and A (A_{ve}) that are relevant to ϵ_f and $E_{\text{gap}}^{\text{der}}$. Here, “vertical” means molecular geometry and hence $v(\mathbf{r})$ do not change upon electron addition or depletion. Meanwhile, many experimental results are referred to as “adiabatic” values (I_{ad} and A_{ad}), where gaining or losing an electron is accompanied with geometry relaxation. Table I summarizes the band-gap related quantities predicted by LDA, B3LYP, MLDA, and their SC-counterparts. The calculations cover atoms H–Ar, molecules in the G2–97 set, and representative solids in Fig. 1.²⁵ Obviously, LDA, B3LYP and MLDA yield reasonable I and A , but they all give considerable errors on ϵ_f . In other words, $E_{\text{gap}}^{\text{int}}$ are obtained accurately, but $E_{\text{gap}}^{\text{der}}$ are severely underestimated. Inclusion of SC significantly improves prediction of ϵ_f while preserving the accuracy of I and A . Among all the DFAs explored in Table I, S-MLDA gives the most accurate $E_{\text{gap}}^{\text{der}}$ with consistent accuracy for systems of all sizes, *i.e.*, from atoms and molecules to solids. Figure 2 compares ϵ_{HOMO} (ϵ_{LUMO}) with $-I_{\text{ve}}$ ($-A_{\text{ve}}$) for all the atoms and molecules studied, where MLDA results display systematic discrepancies between pairs of quantities, which are apparently removed by using S-MLDA.

The quantity of primary significance in the proposed SC method is the Fukui function.

For solids, the apparent linearity condition is satisfied without SC.⁴ The periodic boundary condition requires $f(\mathbf{r}) = 0$, and thus SC has no effect. In contrast, for finite systems $f(\mathbf{r}) \approx |\phi_f(\mathbf{r})|^2$, and linearity condition is restored by SC.

An important application of SC is prediction of size-dependent effect on band gaps of nanostructures, which has remained formidable in DFT. For instance, the quantitative relation between band gap and Si nanoparticle size has been studied extensively,^{26,27} as it highlights the significance of quantum confinement. GW method²⁸ has been used to predict $E_{\text{gap}}^{\text{der}}$ through the quasiparticle orbital energies.²⁹ Reasonable $E_{\text{gap}}^{\text{int}}$ have been obtained by DFT–LDA for small size clusters, but not for large ones.²⁶ $E_{\text{gap}}^{\text{der}}$ by LDA suffer from considerable delocalization error, which is expected to be removed by SC.

We calculated $E_{\text{gap}}^{\text{der}}$ of H-passivated Si nanoparticles of various diameters (d). Computational details are provided in Ref. 19. The $E_{\text{gap}}^{\text{der}}(d)$ obtained by S–LDA correctly reproduces $E_{\text{gap}}^{\text{int}}$ by LDA as reported in Ref. 26; see Fig. 3. This confirms the efficacy of SC on removing delocalization error at fractional occupation. Analogously, SC enlarges the MLDA gaps, and $E_{\text{gap}}^{\text{der}}$ by S–MLDA agree well with the GW results.²⁹ Noting that S–MLDA predicts more accurate $E_{\text{gap}}^{\text{der}}$ than S–LDA for both SiH_4 ($d \rightarrow 0$) and bulk Si ($d \rightarrow \infty$),¹⁹ we believe the S–MLDA prediction to be most reliable at any finite d . As it also inherits from MLDA the capability of predicting thermodynamic properties with similar or better accuracy than GGA,¹⁹ S–MLDA provides a useful tool to characterize quantitatively the size-dependent effects on physical properties of nanostructures. Stein *et al.* proposed a generalized KS method to improve $E_{\text{gap}}^{\text{der}}$ by optimizing the range-separation parameter μ for every system.³⁰ Our SC method is conceptually different, and no tuning of parameter is required. For S–MLDA, the same value of μ is applied to all systems.

The significant improvement on band-gap prediction across system sizes achieved by the SC affirms the understanding that it is useful to characterize DFT errors in the perspective of fractional charges.³¹ The present SC method corrects the delocalization error in energy derivatives for systems with integer electron numbers, using density matrix as a basic variable. We believe this is a key step forward in the direction of correcting the delocalization error in energy for systems with integer electron numbers, which is necessary to improve the prediction of thermodynamic properties in DFT.

Financial support from the Naval Research Office (N00014-09-0576) (XZ, WY), National Science Foundation (CHE-09-11119) (XH, WY), Royal Society (AJC), and Ramón y Cajal

(PMS) is gratefully appreciated.

- ¹ J. P. Perdew, R. G. Parr, M. Levy, and J. L. Balduz, *Phys. Rev. Lett.* **49**, 1691 (1982).
- ² A. J. Cohen, P. Mori-Sánchez, and W. Yang, *Phys. Rev. B* **77**, 115123 (2008).
- ³ W. Kohn and L. J. Sham, *Phys. Rev.* **140**, A1133 (1965).
- ⁴ P. Mori-Sánchez, A. J. Cohen, and W. Yang, *Phys. Rev. Lett.* **100**, 146401 (2008).
- ⁵ P. Mori-Sánchez, A. J. Cohen, and W. Yang, *J. Chem. Phys.* **125**, 201102 (2006).
- ⁶ A. D. Becke, *J. Chem. Phys.* **98**, 5648 (1993).
- ⁷ C. Adamo and V. Barone, *J. Chem. Phys.* **110**, 6158 (1999).
- ⁸ J. Heyd, G. E. Scuseria, and M. Ernzerhof, *J. Chem. Phys.* **118**, 8207 (2003).
- ⁹ T. M. Henderson, A. F. Izmaylov, G. E. Scuseria, and A. Savin, *J. Chem. Phys.* **127**, 221103 (2007).
- ¹⁰ E. R. Johnson, P. Mori-Sánchez, A. J. Cohen, and W. Yang, *J. Chem. Phys.* **129**, 204112 (2008).
- ¹¹ J. P. Perdew and A. Zunger, *Phys. Rev. B* **23**, 5048 (1981).
- ¹² O. A. Vydrov and G. E. Scuseria, *J. Chem. Phys.* **121**, 8187 (2004).
- ¹³ A. J. Cohen, P. Mori-Sánchez, and W. Yang, *J. Chem. Phys.* **126**, 191109 (2007).
- ¹⁴ T. Tsuneda, J.-W. Song, S. Suzuki, and K. Hirao, *J. Chem. Phys.* **133**, 174101 (2010).
- ¹⁵ D. M. Bylander and L. Kleinman, *Phys. Rev. B* **41**, 7868 (1990).
- ¹⁶ H. Iikura, T. Tsuneda, T. Yanai, and K. Hirao, *J. Chem. Phys.* **115**, 3540 (2001).
- ¹⁷ P. M. W. Gill, R. D. Adamson, and J. A. Pople, *Mol. Phys.* **88**, 1005 (1996); A. Savin, in *Recent Developments and Applications of Modern Density Functional Theory*, edited by J. M. Seminario, page 327, Elsevier, Amsterdam, 1996; T. Yanai, D. P. Tew, and N. C. Handy, *Chem. Phys. Lett.* **393**, 51 (2004).
- ¹⁸ S. H. Vosko, L. Wilk, and M. Nusair, *Can. J. Phys.* **58**, 1200 (1980).
- ¹⁹ Supporting Information.
- ²⁰ F. Tran and P. Blaha, *Phys. Rev. Lett.* **102**, 226401 (2009).
- ²¹ M. K. Y. Chan and G. Ceder, *Phys. Rev. Lett.* **105**, 196403 (2010).
- ²² R. G. Parr and W. Yang, *J. Am. Chem. Soc.* **106**, 4049 (1984).
- ²³ K. Takatsuka, T. Fueno, and K. Yamaguchi, *Theor. Chim. Acta* **48**, 175 (1978).

- ²⁴ V. N. Staroverov and E. R. Davidson, *Chem. Phys. Lett.* **330**, 161 (2000).
- ²⁵ L. A. Curtiss, P. C. Redfern, K. Raghavachari, and J. A. Pople, *J. Chem. Phys.* **109**, 42 (1998).
- ²⁶ S. Ögüt, J. R. Chelikowsky, and S. G. Louie, *Phys. Rev. Lett.* **79**, 1770 (1997).
- ²⁷ T. van Buuren, L. N. Dinh, L. L. Chase, W. J. Siekhaus, and L. J. Terminello, *Phys. Rev. Lett.* **80**, 3803 (1998).
- ²⁸ M. S. Hybertsen and S. G. Louie, *Phys. Rev. B* **34**, 5390 (1986).
- ²⁹ M. L. Tiago and J. R. Chelikowsky, *Phys. Rev. B* **73**, 205334 (2006).
- ³⁰ T. Stein, H. Eisenberg, L. Kronik, and R. Baer, *Phys. Rev. Lett.* **105**, 266802 (2010).
- ³¹ A. J. Cohen, P. Mori-Sánchez, and W. Yang, *Science* **321**, 792 (2008).
- ³² R. G. Pearson, *Inorg. Chem.* **27**, 734 (1988).

	MAE	MLDA	S-	LDA	S-	B3LYP	S-
atom	I (18)	0.16	0.16	0.30	0.30	0.20	0.20
	A (15)	0.25	0.25	0.27	0.27	0.12	0.12
	ϵ_{H} (18)	3.53	0.33	5.18	0.33	3.88	0.35
	ϵ_{L} (15)	2.47	0.54	3.33	0.65	2.28	0.67
mole.	I_{ad} (70)	0.22	0.22	0.21	0.21	0.16	0.16
	A_{ad} (47)	0.25	0.25	0.24	0.23	0.13	0.13
	ϵ_{H} (70)	3.10	0.21	4.19	0.35	3.09	0.31
	ϵ_{L} (47)	2.78	0.27	3.66	0.34	2.59	0.39
sol.	E_{gap} (18)	0.77	0.77	1.81	1.81	0.99	0.99

TABLE I: Summary of MAEs in eV. Numbers of species calculated are given in parantheses. “S-” is short for scaled DFA. ϵ_{HOMO} (ϵ_{LUMO}) are compared to calculated I_{ve} (A_{ve}), and others are compared to experimental values.^{25,32}

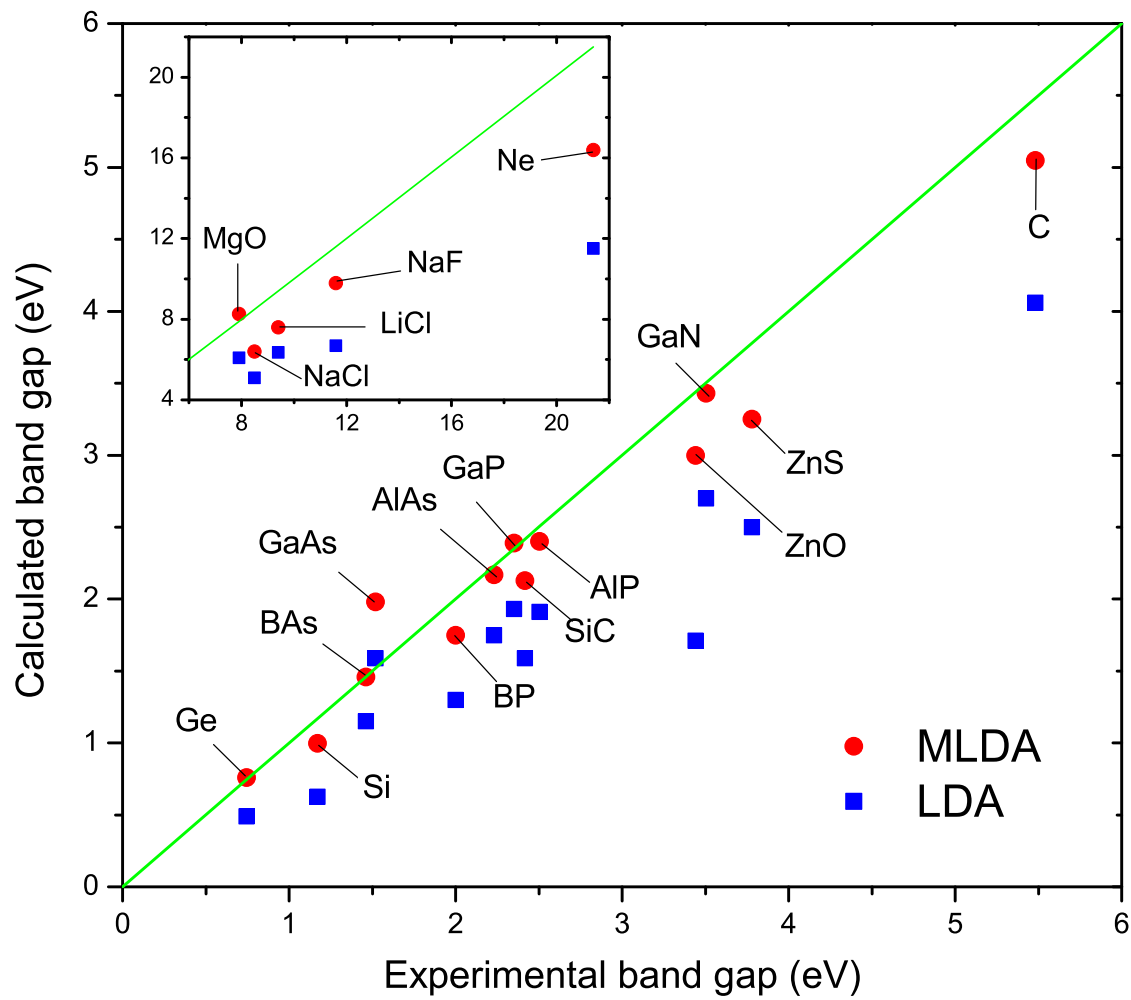


FIG. 1: Calculated versus experimental band gaps of a variety of nonmetallic solids. See Ref. 19 for details.

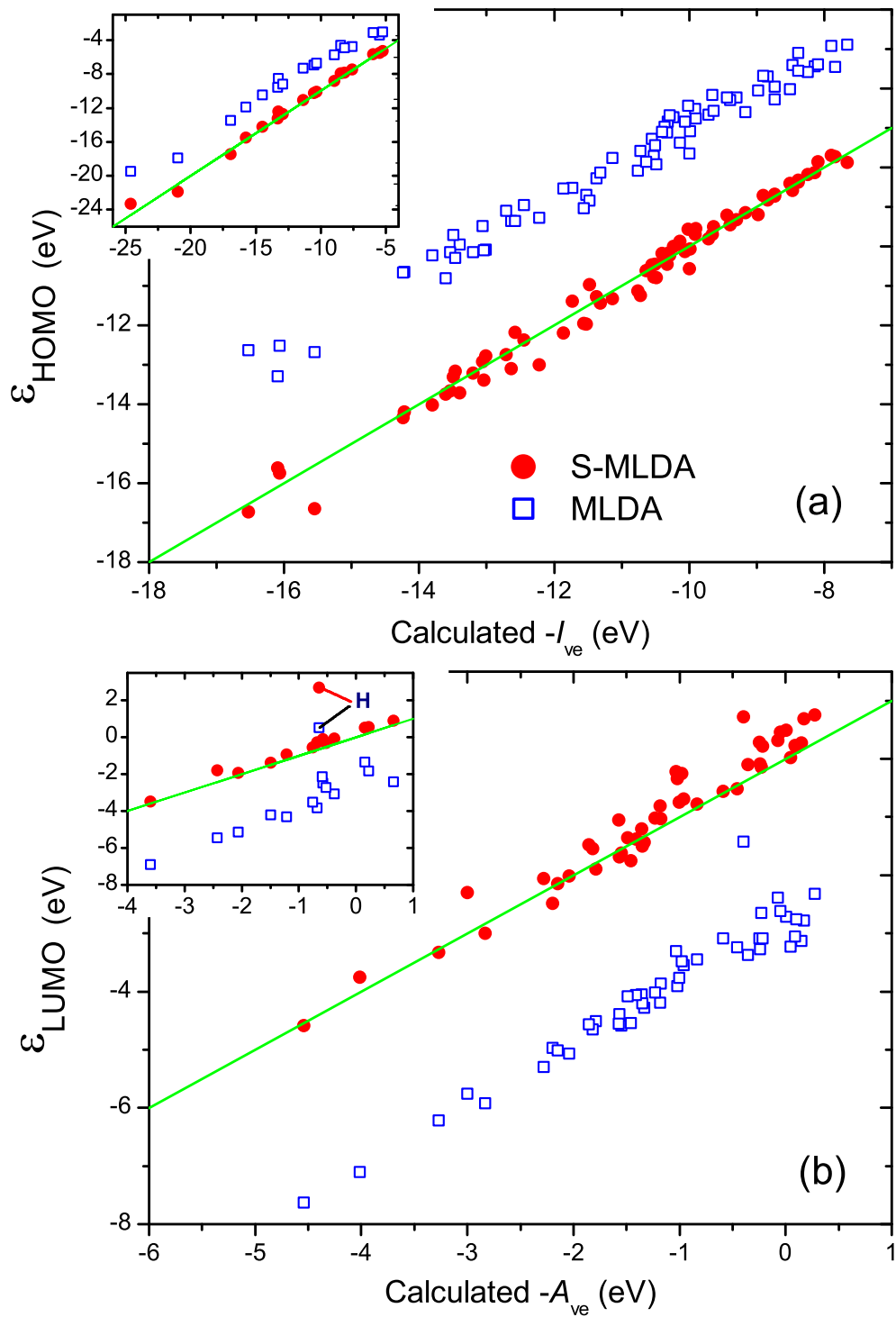


FIG. 2: (a) Calculated ϵ_{HOMO} versus $-I_{\text{ve}}$ for 70 molecules (b) ϵ_{LUMO} versus $-A_{\text{ve}}$ for 47 molecules from G2-97 set. Data for atoms H–Ar are shown in the insets, but without He, Ne, and Ar in inset of (b). The solid line indicates $\epsilon_{\text{HOMO}} = -I_{\text{ve}}$ in (a) and $\epsilon_{\text{LUMO}} = -A_{\text{ve}}$ in (b).

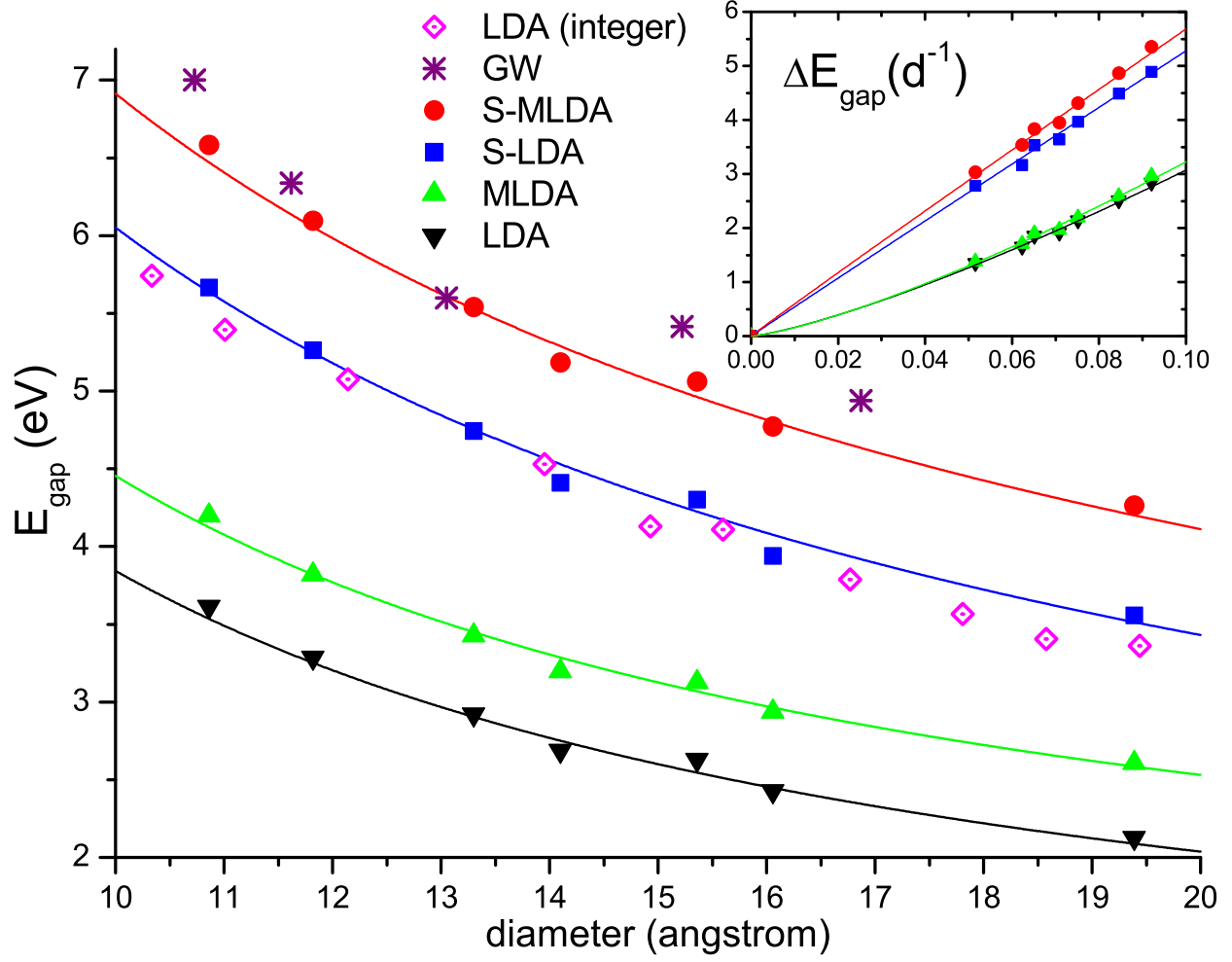


FIG. 3: $E_{\text{gap}}^{\text{der}}$ of H-passivated Si nanoparticles. The LDA and GW predicted $E_{\text{gap}}^{\text{int}}$ are extracted from Refs. 26 and 29. The inset depicts $\Delta E_{\text{gap}}(d) = E_{\text{gap}}^{\text{der}}(d) - E_{\text{gap}}(\text{bulk})$. It is fitted to $\Delta E_{\text{gap}}(d) \approx a(d^{-1})^b$, with $b = 1.28, 0.99, 1.31,$ and 0.98 for LDA, S-LDA, MLDA, and S-MLDA, respectively.